# Lecture 9: 3.2 Qubit state control and readout

*This lecture will be based on references [1], [2], [3].*

## 0 Introduction

In this lecture we will enter the coherent control of superconducting qubits. The first section will study the interaction between a two-level atom and an oscillating field, leading to Rabi oscillations and all the single-qubit gate control. The second section will introduce the quantized version of atom-field interactions in the celebrated Jaynes-Cummings model. This model will enable the dispersive readout technique which is of uttermost important in current superconducting quantum circuits. Finally, we will conclude with qubit-qubit interactions of different types, direct geometric, indirect mediated, etc. that will lead to 2-qubit gates. Together, the lecture will conclude with an overview of implemented quantum algorithms.

## 1 Single qubit state control

### 1.1 Atom-field semiclassical interactions

Controlling a qubit is equivalent to controlling a two-level atom, which requires interacting with it through resonant radiation by application of external oscillating fields. Assuming the external field to contain on average a large number of photons, we can treat it in the semiclassical approximation. Let us take an electric field in a 1D cavity along the $z$-axis in a coherent state, which is the quantum state generated in an microwave source or a laser:

$$\langle \hat{E}(x,t) \rangle = 2|\alpha| \sqrt{\frac{\hbar\omega}{\epsilon_0 V}} \cos(\omega t - kz - \theta) \approx E_0 \cos(\omega). \tag{1}$$

We have assumed the field amplitude to remain constant throughout. Also, for simplicity, we took $\alpha$ as real, $\theta = 0$, and the field in a fixed position (eliminating the $z$ coordinate dependence). Now assume this oscillating field to interact with an electric dipole from an atom $\hat{\vec{d}}_e = q\hat{\vec{r}}$ via dipole interaction,

$$U_d = -\hat{\vec{d}}_e \cdot \hat{\vec{E}} = q\hat{\vec{r}} \cdot \hat{\vec{E}}_0 \cos(\omega t). \tag{2}$$

The dipole operator is an odd function. Therefore, the dipole matrix elements of a two-level system are off-diagonal since, by parity symmetry, $\langle 0|q\hat{\vec{r}}|0\rangle = \langle 1|q\hat{\vec{r}}|1\rangle = 0$,

and $\langle 1|q\hat{\vec{r}}|0\rangle = \langle 0|q\hat{\vec{r}}|1\rangle = |d_e|$. The dipole operator takes then the form $\hat{\vec{d}}_e = |d_e|\hat{\sigma}_x$, which leads to the dipole interaction

$$U_d = |d_e|E_0\cos(\omega t)\hat{\sigma}_x = \hbar\Omega_R\cos(\omega t)\hat{\sigma}_x, \tag{3}$$

where we defined the Rabi frequency $\Omega_R \equiv |d_e|E_0/\hbar$.

Applying this field to the two-level system leads to the Hamiltonian

$$H = \frac{\hbar\omega_q}{2}\hat{\sigma}_z + \hbar\Omega_R\cos(\omega t)\hat{\sigma}_x. \tag{4}$$

In this case we are omitting the self-energy of the field, as we consider it to be a constant. The procedure to solve this problem is by considering a wave function dependent on time $|\psi(t)\rangle = c_0(t)|0\rangle + c_1(t)|1\rangle$ and apply it to the Schroödinger equation with the previous Hamiltonian. This leads to two coupled differential equations for the coefficients $c_0(t)$ and $c_1(t)$. One approximation here is necessary to yield an analytic expression to the coefficients, which is known as the rotating-wave approximation. The idea is to decomponse the cosine as $\cos(\omega t) = (e^{i\omega t} + e^{-i\omega t})/2$ and approximate it as a rotating wave, that is, to move in the frame co-rotating with one of the two components and neglect the other component as it will be oscillating at $2\omega$. That is, $\cos(\omega t) \approx e^{i\omega t}/2$. In the rotating frame of the driving field, obtained by rotating the Hamiltonian in Eq. (4) by $U = e^{i\omega t\sigma_z}$ as

$$H_q^{rot} = UHU^{-1} - i\hbar U\partial U^{-1}/\partial t, \tag{5}$$

since $U$ is time-dependent. The Rabi Hamiltonian becomes

$$H_q^{rot} = \frac{\hbar(\omega_q - \omega)}{2}\hat{\sigma}_z + \frac{\hbar\Omega_R}{2}\hat{\sigma}_x. \tag{6}$$

Here we see the effect of the rotating-wave approximation, which is to remove the explicit time dependence in the Hamiltonian. This rotating frame shows that the applied field behaves like an orthogonal field in the $x$-axis applied to the qubit, that can be visualized as a spin-1/2 oriented in a static magnetic field in the $z$-axis.

The solution to this so-called Rabi problem leads to the probability of the atom to be in the ground state as

$$P_0(t) = |c_0(t)|^2 = \frac{\Omega_r^2}{(\omega_q - \omega)^2 + \Omega_R^2}\cos^2[(\Omega_R^2 + (\omega_q - \omega)^2)^{1/2}\frac{t}{2}]. \tag{7}$$

This is known as the Rabi formula and states that the atom state will evolve from the ground state into the excited state and back, oscillating at a frequency given by $(\Omega_R^2 + (\omega_q - \omega)^2)^{1/2}/2$. When the oscillating field is resonant with the qubit, $\omega = \omega_q$, the oscillation amplitude is complete, and the oscillation frequency becomes identically the Rabi frequency $\Omega_R/2$ (cf. Eq. (6)), hence its name. Stopping the oscillation at time $T = \pi/\Omega_R$ fully inverts the population into $|1\rangle$. We call this a '$\pi$' pulse.

In real qubits, we have found Hamiltonians of the type

$$H = \frac{\hbar\varepsilon}{2}\hat{\sigma}_z + \frac{\hbar\Delta}{2}\hat{\sigma}_x, \tag{8}$$

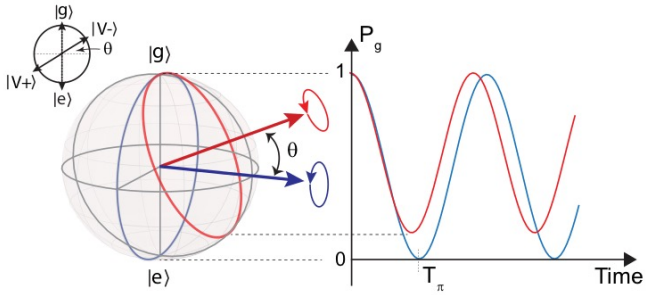


Figure 1: Rabi oscillations of a two-level system.

and the coupling to external fields comes through the $\varepsilon$ coefficient that includes the dipole coupling energy. We can generalize a bit more the Rabi formula by considering an oscillating field with a well-defined phase, $E(t) = E_0 \cos(\omega t + \phi)$. This will result in the interaction term of the Hamiltonian

$$H_{rf} = -\frac{\Omega_R}{2} \cos(\omega t + \phi)\hat{\sigma}_z, \tag{9}$$

This term transforms into the following Hamiltonian in the qubit diagonal basis:

$$H'_{rf} = -\frac{\epsilon}{\omega_q}\frac{\Omega_R}{2} \cos(\omega t + \phi)\hat{\sigma}_z - \frac{\Delta}{\omega_q}\frac{\Omega_R}{2} \cos(\omega t + \phi)\hat{\sigma}_x. \tag{10}$$

Only at the degeneracy point $\epsilon = 0$ this driving is purely transverse. Assuming a resonant drive $\omega = \omega_q$, applying the rotating-wave approximation, and transforming the Hamiltonian to the frame co-rotating at the qubit frequency, $U_R = e^{-i(\omega_q/2)t\sigma_z}$. This results in the final qubit control Hamiltonian

$$H_{rf}" = U_R^\dagger H'_{rf} U_R + \frac{\omega_q}{2}\sigma_z = -\frac{1}{2}\frac{\Delta}{\omega_q}\frac{\Omega_R}{2}(i\cos\phi\hat{\sigma}_x + \sin\phi\hat{\sigma}_y). \tag{11}$$

This Hamiltonian represents an effective transverse field that forces the qubit state to precess, as the qubit eigenbasis is that of $\sigma_z$ and the drive points transverse to it along $\sigma_x$ and $\sigma_y$. Quantum mechanically, we are not anymore in an eigenstate of the qubit+drive combined system, so the state cannot be stationary and oscillates. Another pictures is that of the Bloch sphere, where the field points orthogonal to the state, defining the axis of rotation. This is represented in Fig. 1. We find that by selecting the phase of the driving field $\phi$ we can control the axis of rotation of the qubit in consecutive pulses (because if we apply a single pulse, the value of the phase is irrelevant and can be set to 0).

Implementing this type of control using microwave sources is rather straightforward. A microwave source generates a continuous wave at a given frequency $\omega$, amplitude $A$ and, if it is a stable enough source, phase $\phi$. Therefore, we can select the rotation angle of pulses by selecting the parameter $\phi$ directly at the source.

## 1.2 Single qubit gates

Having obtained a way to control the qubit state and the qubit rotation axis, it is possible to generate any arbitrary state of the qubit by applying the right sequence

of pulses which can be concatenated, having different phase between them and in this way produce a pulse of rotation $\theta$ around axis $\hat{\omega}$. Ideally the qubit state is simply rotated and the final state is reached. However, real-world imperfections make the success probability of this operation, also known as fidelity $\mathcal{F} \equiv |\langle\psi_{\text{target}}|\psi_{\text{final}}\rangle|$, to lie below 100%. Addressing the many imperfections of the system is key to performing high-fidelity single qubit gates.

The very first limitation on performing single-qubit gates is decoherence, or loss of phase coherence and population amplitude. This error can be mitigated by operating long-coherence qubits and fast rotation operations. A several-microsecond coherent qubit driven in a few nanosecond to its target state has a negligible error in the gate.

Superconducting qubits aren't two-level systems and therefore there is a possibility that the qubit population leaks into higher-excited levels. This is particularly worrisome for weakly anharmonic qubits such as the transmon and even the C-shunt flux qubit. The solution to this problem has been found and is known as the DRAG sequency (Derivative Removal by Adiabatic Gate) [4]. This consists of a modulation of the amplitude and phase of the pulse such that the amplitude evolves as a Gaussian, and the phase as the derivative of a Gaussian. This has the effect of creating a destructive interference of the population in the second excited state $|2\rangle$, leading to very high fidelity single-qubit gates.

Further improvement on single-qubit gates is reached by compensating the distortion pulses undergo before they arrive at the sample. Some techniques have been identified to characterize this imperfection and invert it.

Finally, in order to proper characterize single qubit gates, process gate tomography is a common technique. When the number of qubits grows, this becomes impractical as the size of the matrix defining the operation grows very fast. A technique was developed in the ion trap community that has become the standard in characterizing qubit gates known as randomized benchmarking [5], in which a random sequence of $N$ gates is applied to the qubit and eventually it is inverted to lead to the initial state. Experimentally, an exponential decrease of the final state fidelity is seen with the number of gates. This becomes a base line. If one now interleaves another gate between the random pulses, the error produced by the target gate can be separated. This technique is able to distill different sources of error in the gate, such as the readout error, as it provides the average error introduced by the target gate.

# 2 Circuit Quantum Electrodynamics

In order to manipulate the qubit state further without destroying it, and later read it out, many approaches have been tried over the past 2 decades. Eventually, one approach has been finalist, known as circuit quantum electrodynamics, or circuit-QED, in which qubits couple to the electromagnetic field of a resonator, which acts as either the qubit state detector, or the qubit-qubit interaction mediator. This requires going into the fully quantized atom-field model, the Jaynes-Cummings model. This model was originally implemented for atoms and cavities, in the field known as cavity QED, as seen in Fig. 2.

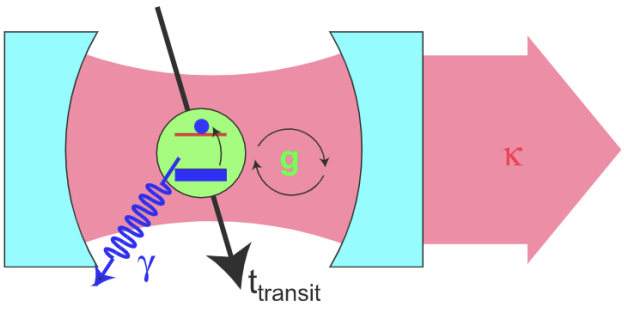


Figure 2: Atom-photon interactions in cavity QED. From [3].

## 2.1 Atom-field quantum interactions

If we consider a two-level atom, or qubit, interacting with a quantized harmonic oscillator, we obtain the following Hamiltonian

$$H = \frac{\hbar\epsilon}{2}\hat{\sigma}_z + \frac{\hbar\Delta}{2}\hat{\sigma}_x + \hbar\omega(\hat{a}^\dagger\hat{a} + 1/2). \tag{12}$$

Normally one would add by hand the atom-field dipole interaction, to yield the cavity-QED-like Hamiltonian. In our case, we use the realistic two-level atom Hamiltonian and derive the dipole interaction from the $\varepsilon$ coefficient. This coefficient will contain a classical part and a quantized part. In the case of the charge qubit, represented in Fig. 3

$$\varepsilon_{CQ} = 8E_C(n_g - 1/2) = 8E_C(-C_gV/2e - 1/2). \tag{13}$$

The voltage is the one containing both contributions: $V = V_0 + \hat{V}$, where $\hat{V}$ is the

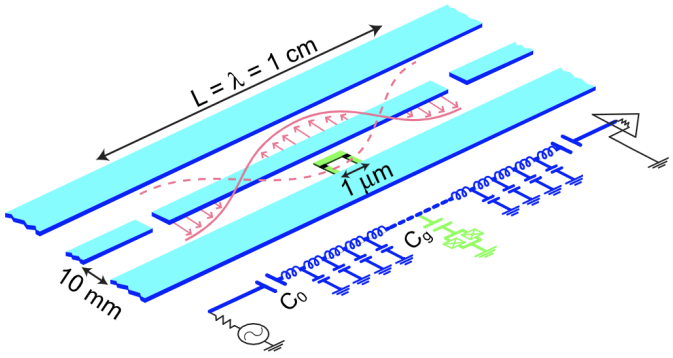


Figure 3: Cooper pair box in a transmission line resonator. From [3].

quantized voltage coming from a single harmonic oscillator mode. Pulling this term outside, leads to the following light-matter Hamiltonian

$$H = \frac{\hbar\epsilon_0}{2}\hat{\sigma}_z + \frac{\hbar\Delta}{2}\hat{\sigma}_x + \hbar\omega(\hat{a}^\dagger\hat{a} + 1/2) - \hbar g\hat{\sigma}_z(\hat{a} + \hat{a}^\dagger). \tag{14}$$

Here we have defined the qubit-field interaction strength $g \equiv 2eV_{\rm rms}(C_g/C_\Sigma)$, where $V_{\rm rms}$ are the zero-point fluctuations of the field mode, even when it is in the vacuum

state. At the symmetry point, and rotating the qubit basis by 90°, the Hamiltonian becomes

$$H = \frac{\hbar\Delta}{2}\hat{\sigma}_z + \hbar\omega(\hat{a}^\dagger\hat{a} + 1/2) - \hbar g\hat{\sigma}_x(\hat{a} + \hat{a}^\dagger). \tag{15}$$

This Hamiltonian is known as the quantum Rabi model, and only in 2011 was finally analytically solved [6]. A much simpler solution can be obtained by considering the following approximation: if the qubit-oscillator system dynamics, governed by their coupling strength $g$ is much slower than the uncoupled resonance frequencies of each subsytem, $\omega_q$ and $\omega$, out of the four interaction terms $\sigma_x(a + a^\dagger) = \sigma_+ a + \sigma_- a^\dagger + \sigma_+ a^\dagger + \sigma_- a$, the latter two that do not conserve the number of excitations can be dropped. In the interaction picture, these terms oscillate at frequencies $\omega_q + \omega$, compared to the other terms oscillating at $\omega_q - \omega$. This is known as the rotating-wave approximation, similarly as in the previous section. Within this approximation, the Hamiltonian becomes the well-known Jaynes-Cummings model

$$H_{\rm JC} = \frac{\hbar\Delta}{2}\hat{\sigma}_z + \hbar\omega(\hat{a}^\dagger\hat{a} + 1/2) - \hbar g(\hat{\sigma}_+\hat{a} + \hat{\sigma}_-\hat{a}^\dagger). \tag{16}$$

This Hamiltonian is used in superconducting qubit circuits, but it was originally derived for single atoms inside optical cavities, the field known as cavity QED. It has also been applied in semiconductor quantum dots in microcavities, and in general is applicable in few-level systems coupled to harmonic resonances.

Note that this Hamiltonian commutes with the number excitation operator $\hat{N} \equiv \hat{\sigma}_z + \hat{a}^\dagger\hat{a}$, $[H_{\rm JC}, \hat{N}] = 0$. Therefore, we can consider subspaces where the excitation number is fixed, since it is a constant of motion, and diagonalize the Hamiltonian within this subspace. We then find the eigenenergies, as represented in Fig 4

$$E_{g,0} = -\frac{\hbar\delta}{2} \tag{17}$$

$$E_{\pm,n} = (n+1)\hbar\omega \pm \frac{\hbar}{2}\sqrt{4g^2(n+1) + \delta^2}, \tag{18}$$

where $\delta \equiv \omega_q - \omega$ is the system detuning. $E_{g,0}$ is the ground state energy of the system in state $|g0\rangle$, where no excitations exist. The energies $E_{\pm,n}$ correspond to the so-called dressed states containing a total of $n$ photon excitations

$$|+,n\rangle = \cos\theta_n|e,n\rangle + \sin\theta_n|g,n+1\rangle \tag{19}$$

$$|-,n\rangle = -\sin\theta_n|e,n\rangle + \cos\theta_n|g,n+1\rangle, \tag{20}$$

with the mixing angle being

$$\tan 2\theta_n = \frac{2g\sqrt{n+1}}{\delta}. \tag{21}$$

When $\delta = 0$ (resonance), the eigenstates become exact superpositions of qubit and photon. The system is contained inside an environment that affects both the qubit as well as the photons in the resonator. Qubit decay is given by $\gamma_q = T_1^{-1}$, while resonator damping is $\kappa$. The system is in the strong coupling regime, where coherent dynamics takes place over dissipative damping, if $g \gg \kappa, \gamma_q$. In this regime, an excitation from the qubit can be resonantly transferred to the empty resonator, in what is known today as vacuum Rabi oscillations, first seen in ref. [7].

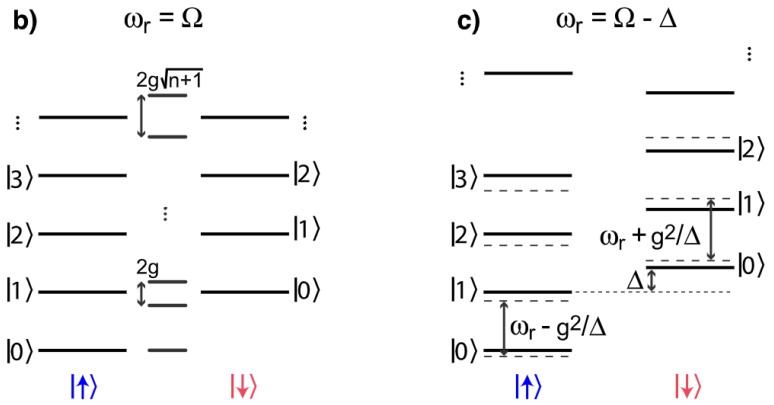


Figure 4: Spectrum of the Jaynes-Cummings model for resonant (left) and dispersive (right) regimes. From [3].

## 2.2 Single qubit dispersive readout

In the so-called dispersive regime, where $\delta \gg g$, the original Jaynes-Cummings Hamiltonian can be transformed with $\hat{U} = e^{(g/\delta)(\hat{a}\hat{\sigma}_+ - \hat{a}^\dagger\hat{\sigma}_-)}$ as

$$\hat{U}H_{\mathrm{JC}}\hat{U}^\dagger \approx \hbar\left[\omega + \frac{g^2}{\delta}\hat{\sigma}_z\right]\hat{a}^\dagger\hat{a} + \frac{\hbar}{2}\left(\omega_q + \frac{g^2}{\delta}\right)\hat{\sigma}_z. \tag{22}$$

This dispersive Hamiltonian is also known as AC-Stark Hamiltonian. We can see the first term as being a modified resonator frequency as function of the qubit state. This shift is known as the AC-Stark shift and is the basis of qubit state readout in a resonator. The second term is the qubit frequency modified by a constant that depends on the presence of the resonator. This term is known as the Lamb shift, and it comes from the vacuum fluctuations inducing a frequency shift in the qubit. Therefore, by reading out the resonator energy, in other words the operator $\hbar\omega\hat{a}^\dagger\hat{a}$, we can determine the expectation value of the qubit operator $\langle\hat{\sigma}_z\rangle$. This is nearly a quantum non-demolition measurement, as the measurement operator commutes with the approximated dispersive Hamiltonian. The higher-order terms introduce a small error which is normally neglected. The shift produced by the qubit on the resonator is known as the dispersive shift, which in the two-level system case is $\pm\chi \equiv g^2/\delta$, the sign depending on whether the qubit is in the excited/ground state. Figure 5 shows the transmitted amplitude and phase of a resonator holding a qubit in its two eigenstates.

In transmon qubits, as the system is weakly anharmonic, the higher levels do play a role, leading to a renormalized $\chi$ of

$$\chi = \chi_{01} - \chi_{12}/2, \tag{23}$$

where

$$\chi_{ij} = \frac{g_{ij}^2}{\omega_{ij} - \omega}. \tag{24}$$

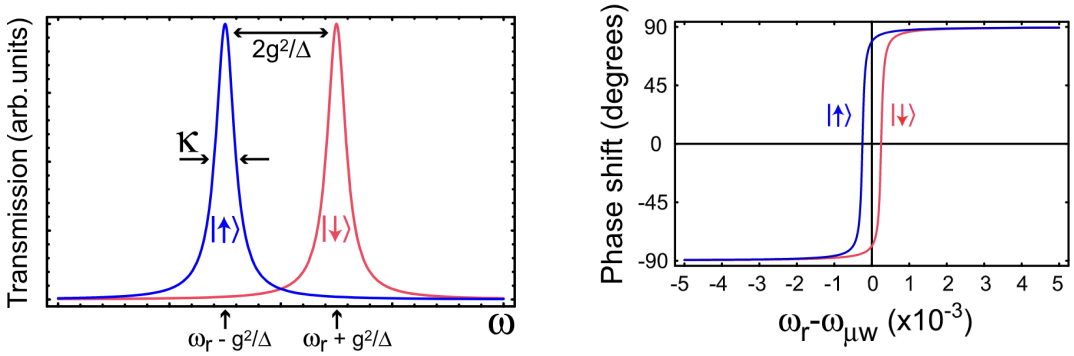


Figure 5: (Left) Measurement readout of the amplitude of the signal in the JC model. (Right) Same but using the phase. From [3].

In practice, one measures the qubit state by proving the resonator at one of its two eigenfrequencies $\omega_\pm = \omega \pm \chi$. A probing pulse of frequency $\omega_p$ when the qubit is in the ground state at $\omega_p = \omega_- = \omega - \chi$ will be transferred through the resonator, yielding a high signal (see Fig. 6). When the qubit becomes excited, the pulse will be off-resonant with $\omega_+$, and the pulse will be reflected, leading to a low signal. This then represents a mapping between 0,1 and high/low signal. One then needs to acquire sufficient statistics to overcome the system noise, and the intrinsic quantum fluctuations in order to perform qubit state tomography.

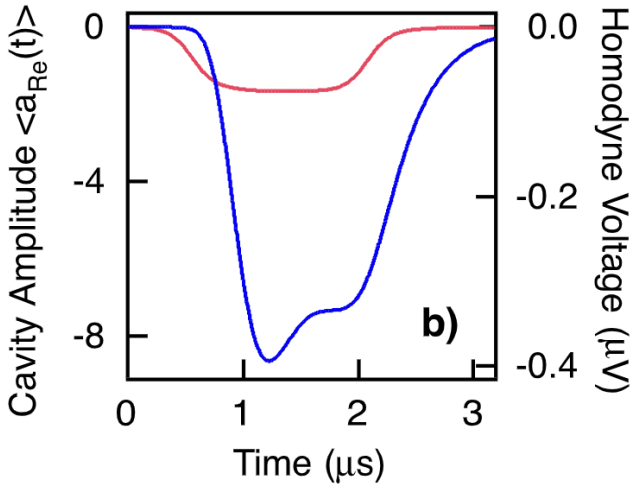


Figure 6: Integrated signal from a resonator depending on the qubit state, showing the two different amplitudes of voltage distinguishing the qubit states $|0\rangle, |1\rangle$. From [3].

The eigenstates of the one excitation maniold in this regime become

$$|-,0\rangle \simeq -(g/\delta)|e,0\rangle + |g,1\rangle, \tag{25}$$
$$|+,0\rangle \simeq |e,0\rangle + (g/\delta)|g,1\rangle. \tag{26}$$

This small but finite entanglement between qubit and resonator leads to the so-called enhanced Purcell decay rate. In particular, the decay rate of each of the two

states is

$$\Gamma_{-,0} \simeq (g/\delta)^2 \gamma_q + \kappa, \tag{27}$$

$$\Gamma_{+,0} \simeq \gamma_q + (g/\delta)^2 \kappa. \tag{28}$$

According to these relations, a detuned qubit in the excited state, will feel an additional decay channel into the resonator mode, with a probability $(g/\delta)^2$. One would want to minimize this quantity by increasing the detuning significantly. Unfortunately, that also reduces $\chi$, and therefore the signal contrast. The optimum can be shown to be $\chi = \kappa/2$ [8]. In order to circumvent this limitation, the UCSB group pioneered a filtering resonator, known as the Purcell filter, that decouples the qubit-resonator readout system from the readout line that injects noise into the system. This additional resonator permits detuning the qubit from the readout resonator by a significant amount without compromising the signal quality.

The terms in the dispersive Hamiltonian can be re-arranged such that

$$\hat{U} H_{\mathrm{JC}} \hat{U}^\dagger \approx \hbar\omega \hat{a}^\dagger \hat{a} + \hbar \left[ \frac{\omega_q}{2} + \frac{g^2}{\delta} \left( \hat{a}^\dagger \hat{a} + \frac{1}{2} \right) \right] \hat{\sigma}_z. \tag{29}$$

In this case, it is the qubit frequency that experiences a shift for every different photon number state $n$. In fact, in the so-called strong dispersive regime where $g^2/\delta \gg \kappa, \gamma_q$, this shift produced by each photon number can be resolved, and the qubit becomes a sensor of single photon states in the resonator.

# References


[1] Krantz, P. *et al.* A quantum engineer's guide to superconducting qubits. *Applied Physics Reviews* **6**, 021318 (2019). URL `https://doi.org/10.1063/1.5089550`. `https://doi.org/10.1063/1.5089550`.

[2] Cohen-Tannoudji, C., Diu, B. & Laloe, F. *Quantum Mechanics, vols. 1 and 2* (John Wiley & Sons, Inc., 1977).

[3] Blais, A., Huang, R. S., Wallraff, A., Girvin, S. M. & Schoelkopf, R. J. Cavity quantum electrodynamics for superconducting electrical circuits: An architecture for quantum computation. *Phys. Rev. A* **69**, 062320 (2004). URL `http://dx.doi.org/10.1103/physreva.69.062320`.

[4] Motzoi, F., Gambetta, J. M., Rebentrost, P. & Wilhelm, F. K. Simple Pulses for Elimination of Leakage in Weakly Nonlinear Qubits. *Physical Review Letters* **103**, 110501+ (2009). URL `http://dx.doi.org/10.1103/physrevlett.103.110501`.

[5] Chow, J. *et al.* Randomized benchmarking and process tomography for gate errors in a solid-state qubit. *Physical Review Letters* **102**, 090502+ (2009). URL `http://dx.doi.org/10.1103/physrevlett.102.119901`.

[6] Braak, D. Integrability of the rabi model. *Phys. Rev. Lett.* **107**, 100401 (2011). URL http://view.ncbi.nlm.nih.gov/pubmed/21981483.

[7] Hofheinz, M. *et al.* Generation of Fock states in a superconducting quantum circuit. *Nature* **454**, 310–314 (2008). URL http://dx.doi.org/10.1038/nature07136.

[8] Gambetta, J. *et al.* Quantum trajectory approach to circuit qed: Quantum jumps and the zeno effect. *Phys. Rev. A* **77**, 012112 (2008). URL https://link.aps.org/doi/10.1103/PhysRevA.77.012112.